Vol. 643: 33–48, 2020
https://doi.org/10.3354/meps13333

MARINE ECOLOGY PROGRESS SERIES
Mar Ecol Prog Ser

Published June 11

Resilience of plankton trophic structure to an eddy-stimulated diatom bloom in the North Pacific Subtropical Gyre

Moira Décima[1,*], Michael R. Landry[2]

[1]National Institute of Water and Atmospheric Research, Hataitai, Wellington 6022, New Zealand
[2]Scripps Institution of Oceanography, University of California San Diego, La Jolla, California 92093, USA

ABSTRACT: We investigated the response of an open-ocean plankton food web to a major ecosystem perturbation event, the Hawaiian lee cyclonic eddy Opal, using compound-specific isotopic analyses of amino acids (CSIA-AA) of individual zooplankton taxa. We hypothesized that the massive diatom bloom that characterized Opal would lead to a shorter food chain. Using CSIA-AA, we differentiated trophic position (TP) changes that arose from altered transfers through protistan microzooplankton, versus metazoan carnivory, and assessed the variability at the base of the food web. Contrary to expectation, zooplankton TPs were higher in the eddy than in ambient control waters (up to 0.8 trophic level), particularly for suspension feeders close to the food-web base. Most of the effect was due to increased trophic transfers through protistan consumers, indicating a general shift up, not down, of grazing and remineralization in the microbial food web. *Eucalanus* sp., which was 15-fold more abundant inside compared to outside of the eddy, was the only taxon observed to be a true herbivore (TP = 2.0), consistent with a high phenylalanine (Phe) $\delta^{15}N$ value indicating feeding on nitrate-fueled diatoms in the lower euphotic zone. *Oncaea* sp., an aggregate-associated copepod, had the largest (1.5) TP difference, and lowest Phe $\delta^{15}N$, suggesting that detrital particles were local hot spots of enhanced microbial activity. Rapid growth rates and trophic flexibility of protistan microzooplankton apparently allow the microbial community to reorganize to bloom perturbations, as microzooplankton remain the primary phytoplankton grazers — despite the dominance of large diatoms — and are heavily preyed on by the mesozooplankton.

KEY WORDS: Compound-specific · Omnivory · Nitrogen · Isotope · Food web · Zooplankton

1. INTRODUCTION

Mesoscale physical phenomena, such as eddies, can have substantial effects on biological interactions and biogeochemistry (Benitez-Nelson et al. 2007, Chenillat et al. 2015, McGillicuddy 2016, Sherin et al. 2018). For instance, the doming isopycnals of cold-core eddies (cyclonic circulation in the Northern Hemisphere) bring high nutrient concentrations into the euphotic zone, often doubling the f-ratios of surrounding waters (Sherin et al. 2018). On the global scale, estimates of eddy-enhanced new production range from 10 to 50% of annual new production (Falkowski et al. 1991, Oschlies & Garcon 1998, Siegel et al. 1999, Benitez-Nelson & McGillicuddy 2008). Eddy perturbations can similarly stimulate the biological carbon pump (e.g. Goldthwait & Steinberg 2008), up to 7-fold higher in the core of the eddy compared to outside (Waite et al. 2016), though not always (Maiti et al. 2008). Enhanced production of higher trophic levels has also been documented, through peaks in zooplankton biomass (Goldthwait & Steinberg 2008, Landry et al. 2008b) and greater growth and survival of larval fishes (Shulzitski et al.

*Corresponding author: moira.decima@niwa.co.nz

2015, 2016). These mesoscale features thus represent complex ocean phenomena with significant impacts on marine food webs and biogeochemistry.

Eddies can also serve as manageable natural experimental systems to evaluate the effects of rapidly altered physical conditions on biological communities and biogeochemical dynamics. Particularly in oligotrophic waters of the central subtropical gyres, perturbation effects can be measured against sparse and relatively constant background communities (McGowan & Walker 1979), and prominent features can be readily tracked by their sea surface characteristics (e.g. satellite sea surface height, temperature, chlorophyll *a*) for repeat sampling and study. One such example was a large cyclonic Hawaiian lee eddy (Opal, see Fig. 2) that formed in waters of the North Pacific Subtropical Gyre (NPSG), south of the Big Island of Hawai'i in February 2005, and was intensively studied several weeks later (Benitez-Nelson et al. 2007). Hawaiian lee eddies spin up reliably during periods of intensifying trade winds, which generate strong wind stress curl in the 'Alenuihāhā channel between the high mountain islands of Maui and Hawai'i (Dickey et al. 2008). Opal was particularly notable in having an isopycnal (nitracline) doming of ~100 m in its central region, stimulating a massive deep-euphotic-zone bloom of large diatoms from which it got its name (Benitez-Nelson et al. 2007). Experimental studies conducted in Opal and in ambient 'control' waters documented large increases in nutrient delivery, phytoplankton/zooplankton biomass, primary production and grazing (Benitez-Nelson et al. 2007, Brown et al. 2008, Landry et al. 2008a,b, Rii et al. 2008), and provide an unprecedented dataset on general food-web relationships during the late bloom decline.

In this study, we used compound-specific isotopic analyses of amino acids (CSIA-AA) of individual zooplankton taxa to investigate trophic differences within and outside of eddy Opal. We estimated the contribution of protistan and metazoan heterotrophs to metazoan zooplankton, and determined changes in the baseline phytoplankton supporting zooplankton consumers. Based on conventional understanding of the differences expected, for example, between trophic structure in coastal diatom blooms versus that in picophytoplankton-dominated oligotrophic waters (e.g. Legendre & Rassoulzadegan 1995), we hypothesized that the bloom of large phytoplankton would lead to a shorter food chain with lower average trophic positions (TPs) of zooplankton. This arises because most mesozooplankton cannot directly consume very small (<2 µm) phytoplankton (Hansen et al. 1994) and consequently rely on intermediate trophic levels of protistan microzooplankton as their primary food resource in the open ocean (Calbet & Landry 1999, Calbet & Saiz 2005, Calbet 2008). In principle, the presence of abundant large diatoms should decrease the importance of the picophytoplankton–protistan grazer–mesozooplankton trophic pathway and lead to an increase in the diatom–mesozooplankton grazer food chain, thus altering the major route of carbon and nitrogen flow in this oceanic ecosystem.

CSIA-AA is a technique that uses the measured differences in $\delta^{15}N$ values of different types of AAs within the body tissue of a consumer. The 'trophic' AAs enrich strongly with each trophic transfer, and the 'source' AAs remain similar to source N at the base of the food web. The difference in $\delta^{15}N$ of these 2 groups allows the calculation of the consumer's mean TP (Hannides et al. 2009). Because CSIA-AA was very new to the marine science field when cyclonic eddy Opal was initially investigated, it was not part of the methods planned to be used in the study. Nonetheless, we sorted specimens from the preserved zooplankton samples and analyzed them for CSIA-AA relatively soon (2008) thereafter. For most of the intervening decade between these analyses and the present, a key issue in CSIA-AA interpretation has been the extent to which trophic AAs reveal different aspects of a consumer's food web linkages. The commonly used trophic AA glutamic acid (Glu), for example, has been shown to account only for the metazoan steps in the food web, while alanine (Ala) accounts for both metazoan and protistan microzooplankton steps (Gutiérrez-Rodríguez et al. 2014, Décima et al. 2017). Here, we used both Glu and Ala as trophic AAs in conjunction with the source AA phenylalanine (Phe) to highlight differences in trophic structure that arise primarily from changes in the number of steps through protistan consumers as compared to changes in carnivory (feeding on metazoan prey). As schematically illustrated in Fig. 1, a zooplankter that feeds exclusively on phytoplankton will be seen as a herbivore (TP = 2) by both Glu and Ala, whereas one that feeds on an intermediate level of herbivorous protists will show a 1-step difference between TP_{Ala} and TP_{Glu}. Such differences occurring at the base of the food web will also propagate to higher-level consumers.

Finally, we used these diagnostics to provide new insights on trophic-space differences that exist among taxa. Niche diversification in the marine pelagic occurs primarily over the vertical dimension, as most factors (e.g. food and predation) co-vary with depth.

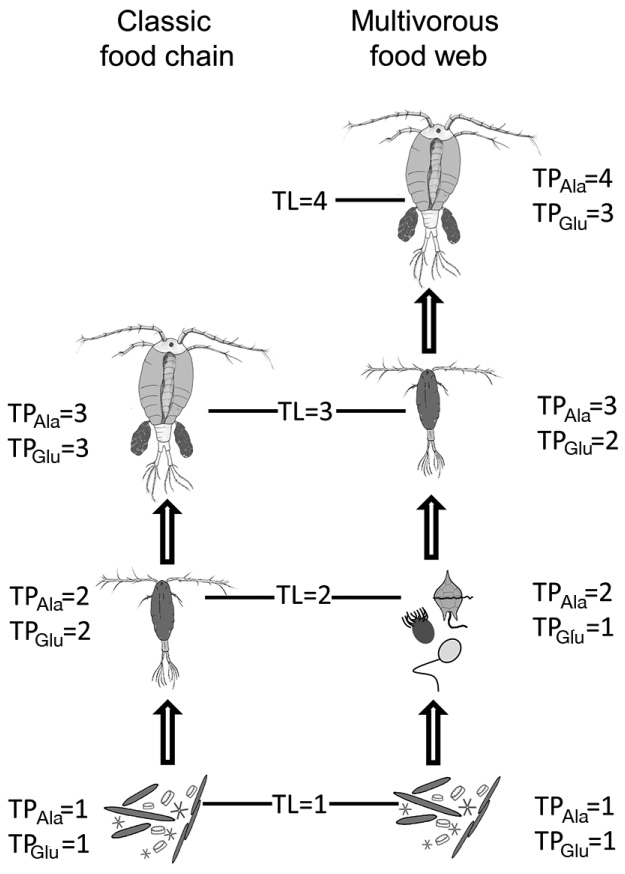

Fig. 1. Schematic depiction of the different trophic positions (TPs) indicated by TP_{Glu} and TP_{Ala}. TL refers to a zooplankter's actual trophic level, and the TP_{Ala}/TP_{Glu} indicates what each amino acid-based trophic index captures (i.e. including/not including protistan consumers). These examples correspond to idealized scenarios of the 'classical food chain,' and the 'multivorous food web,' where the latter includes protistan grazers on phytoplankton and the former does not. TP_{Ala} and TP_{Glu} are equal (left side) if protistan microzooplankton are not part of the food chain, and mesozooplankton are the main consumers of phytoplankton. TP_{Ala} exceeds TP_{Glu} (right side) to the extent that reflects the mean number of trophic steps occupied by protistan microzooplankton in the food chain leading to mesozooplankton

We investigated whether trophic differences existed among 4 congeners of the genus *Pleuromamma*, that are largely thought to share the same habitat, based on previous studies. Trophic differences could specify different ecological niches for each *Pleuromamma* species not evident in the physical environment, as they overlap in vertical distributions, and could explain the co-existence of these 4 sibling species over similar depth ranges.

2. MATERIALS AND METHODS

2.1. Zooplankton sampling

Zooplankton samples were collected from the central region of Opal on the E-Flux III cruise on RV 'Wecoma' between 16 and 21 March 2005 (Fig. 2). Comparable samples were taken from other stations well removed from the eddy influence from 24 to 26 March 2005. As described by Landry et al. (2008b), all samples were taken with oblique tows of a 1 m^2 net with 200 µm Nitex mesh, a General Oceanics flowmeter to measure volume filtered, and a Brancker model XL-200 temperature–pressure recorder to measure tow depth. The mean ± SD tow depth of 166 ± 24 m included the full euphotic zone, which varied between 90 and 140 m as defined by the depth of penetration of 0.5% incident solar radiation. Half of the net codend contents was preserved in 4% buffered formalin, and the other half was processed for size-fractioned estimates of zooplankton biomass and gut fluorescence/grazing, as reported previously (Landry et al. 2008b).

2.2. Sample processing for CSIA-AA

Groups of specimens for CSIA-AA were obtained from the formalin-preserved samples. Prior to sorting, the zooplankton samples had been preserved in formalin for 3 yr. For most of the taxa analyzed, including appendicularians, the euphausiid *Stylo-*

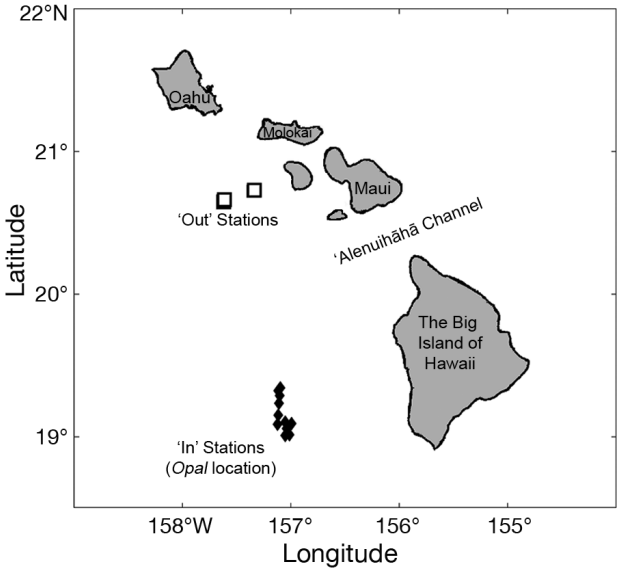

Fig. 2. Study region located in the lee of the Big Island of Hawai'i (USA). Black diamonds are stations samples inside the cylonic eddy Opal, white squares are stations outside of Opal

cheiron carinatum, and the copepods *Pleuromamma abdominalis, P. gracilis, Euchaeta rimana, Lucicutia flavicornis, Mecynocera clausii* and *Oncaea* sp., we sorted comparable samples from net collections made both within ('In') and outside ('Out') of the eddy (Table 1). In addition, we assayed several taxa, namely the copepod *Eucalanus* sp., including adults and copepodites (cop.), and *Oithona* sp. from In stations only, and *P. xiphias* and *P. piseki* from Out stations only, that were sufficiently abundant at In or Out stations, but not both. The number of individuals assayed varied with taxon, averaging 20 specimens per group for the larger species (e.g. *E. rimana*) and up to 200 individuals for the smaller *Oithona* sp. The sorted zooplankton were rinsed in Milli-Q water and dried at 60°C for 24 h prior to chemical preparation for CSIA-AA.

2.3. Hydrolysis and sample derivatization

We followed the procedures for sample preparation of CSIA-AA as described previously (see Hannides et al. 2009, Décima et al. 2013). Acid hydrolysis of AAs, esterification of the terminal carboxyl groups and trifluoroacetylation of the amine groups are the 3 major steps involved (Macko et al. 1997). We hydrolyzed the samples with Sequanal grade 6 N hydrochloric acid to each vial containing sample (~1 mg zooplankton dry weight, DW). Vials were flushed with N_2, capped with a Teflon-lined cap, and heated at 150°C for 70 min. Tryptophan and cystine were not recovered because acid hydrolysis destroys these AAs. In addition, hydrolysis converts asparagine to aspartic acid and glutamine to glutamic acid. The hydrolysate was dried under a stream of N_2 at 55°C, redissolved in 1 ml 0.01 N HCl, purified by filtration using 0.45-µm hydrophilic filter, and washed with 1 ml of 0.01 N HCL. We purified the hydrolysate using cation-exchange chromatography with a 50 mm column of resin (Dowex 50WX8-400) prepared in a glass Pasteur pipette (Metges et al. 1996). The AAs were eluted with 4 ml of 2 N NH_4OH and dried under N_2 at 80°C. We reacidified the samples with 500 µl of 0.2 N HCl, flushed with N_2, heated to 110°C for 5 min and evaporated to dryness under N_2 at 55°C. Esterification of hydrolyzed samples was done with 2 ml of 4:1 isopropanol:acetyl chloride, flushed with N_2 and heated to 110°C for 60 min. Samples were dried at 60°C under N_2, then acylated by adding 1 ml of 3:1 methylene chloride:trifluoracetic anhydride (TFAA) and heated to 100°C for 15 min. Purification of derivatized AAs was done by solvent extraction, following Ueda et al. (1989). Evaporation of acylated AA esters was done at room temperature, under a stream of N_2, and redissolved in 3 ml of 1:2 chloroform:P-buffer (KH_2PO_4 + Na_2HPO_4 in Milli-Q water, pH 7). We ensured that the derivitized AAs were partitioned into chloroform, and that contaminants remained in the P-buffer, through vigorous shaking. Centrifugation (10 min at 600 × *g*) was done to separate both solvents, the chloroform was transferred to a clean vial, and the solvent extraction process was repeated. The acylation step was repeated to ensure derivatization. Samples were stored at −20°C in 3:1 methylene chloride:TFAA for up to 6 mo until isotope analysis.

Table 1. Zooplankton species/genera inside (In) and outside (Out) of eddy Opal, with 'x' indicating that the group was sorted and assayed for compound-specific isotopic analyses of amino acids

Species/genus	In	Out
Appendicularia	x	x
Eucalanus sp. (adults)	x	
Eucalanus spp. copepodites	x	
Euchaeta rimana	x	x
Lucicutia flavicornis	x	x
Mecynocera clausii	x	x
Oithona spp.	x	
Oncaea spp.	x	x
Pleuromamma abdominalis	x	x
Pleuromamma gracilis	x	x
Pleuromamma piseki		x
Pleuromamma xiphias		x
Stylocheiron carinatum	x	x

2.4. CSIA-AA

The TFAA derivatives of AAs were analyzed by isotope ratio monitoring gas chromatography-mass spectrometry. A Delta V Plus mass spectrometer (Thermo Scientific™) was used interfaced with a Trace GC gas chromatograph through a GC-C III combustion furnace (980°C), reduction furnace (650°C), and liquid nitrogen cold trap. An aliquot (1 to 2 µl) of each sample was injected (split/splitless injector, split ratio 10:1) onto a forte BPx5 capillary column (30 m × 0.32 mm × 1.0 µm film thickness) at an injector temperature of 180°C, with a helium flow rate of 1.4 ml min^{-1}. We held the column temperature initially at 50°C for 120 s and then increased to 190°C at a rate of 8°C min^{-1}. When the temperature reached 190°C, it was further increased at a rate of 10°C min^{-1} to 300°C, where it was held for 7.5 min. Aminoadipic

acid and norleucine of known nitrogen isotopic composition were co-injected with samples as internal reference compounds, and used to normalize the measured $\delta^{15}N$ values of unknown AAs. Samples were analyzed in triplicate, except for *E. rimana* (Out sample), where not all runs yielded data above the acceptable chromatographic threshold. The standard deviations for multiple runs of AAs averaged 0.57‰, ranging between 0.02 and 2.4‰.

2.5. TP calculations

AAs were classified into 2 classes following Hannides et al. (2009). Trophic AAs include: alanine (Ala), aspartic acid (Asp), glutamic acid (Glu), isoleucine (IsoL), leucine (Leu), proline (Pro) and valine (Val). Source AAs are: glycine (Gly), lysine (Lys), phenylalanine (Phe), serine (Ser) and threonine (Thr). We calculated TPs in 2 ways: using Glu (TP_{Glu}) as the trophic AA to estimate the trophic transfers involving only metazoan consumers, and using Ala (TP_{Ala}) as the trophic AA to include transfers through both protistan and metazoan (Décima et al. 2017) consumers. Phe was used as the source AA in both cases (Table S1 & S2 in the Supplement at www.int-res.com/articles/suppl/m643p033_supp.pdf). The general equation for the TP calculations is:

$$TP_{Tr} = (\delta^{15}N_{Tr} - \delta^{15}N_{Phe} - \beta) / TEF + 1 \quad (1)$$

where Tr corresponds to Glu or Ala, β is the difference between Tr (Glu or Ala) and Phe in primary producers (β_{Glu} = 3.4‰; β_{Ala} = 3.2‰), and TEF is the trophic enrichment factor, which accounts for the enrichment in AA ^{15}N with each trophic step (TEF_{Glu} = 6.1‰; TEF_{Ala} = 4.5‰). The TEFs used were derived from field-based regressions (Bradley et al. 2015) and multi-step laboratory-experiments (Décima et al. 2017) and are lower than those used by Chikaraishi et al. (2009). The latter are based on pure herbivory of laboratory monocultures and have been shown to overestimate the TEFs of field-collected animals feeding on mixed diets (Hoen et al. 2014, Bradley et al. 2015, Nielsen et al. 2015, Décima et al. 2017, Landry & Décima 2017).

The time-integrated trophic contribution of the protistan food web was quantified using the difference between the 2 trophic indices, and is indicated by

$$\Delta TP = TP_{Ala} - TP_{Glu} \quad (2)$$

Finally, we estimated microzooplankton (µzoo) TP and their likely contribution to the diet of mesozooplankton (mesoZ). In principle, the TP of each zooplankter is given by the sum of the dietary fraction (DF) of each µzoo and mesoZ prey (*i*) multiplied by the prey TP*i*, as delineated in the equations below:

$$TP_{Glu} = 1 * DF_{phyto+\mu zoo} + \left(\sum_i TP_{Glu_{meso_i}} * DF_{meso_i} \right) + 1 \quad (3)$$

$$TP_{Ala} = 1 * DF_{phyto} + \left(\sum_i TP_{Ala_{\mu zoo_i}} * DF_{\mu zoo_i} \right) + \left(\sum_i TP_{Ala_{mesoZ_i}} * DF_{mesoZ_i} \right) + 1 \quad (4)$$

However, this system of equations is underdetermined, as there are more variables than equations to constrain them. Our current CSIA-AA approach allows us only to determine the value of the product of TP×DF for each prey type (µzoo or mesoZ). To investigate the range of possible contributions of µzoo to zooplankton taxa, we used the simplified equations below and calculated this for *Eucalanus*, a representative mesozooplankton grazer at the bottom of the food web. Note that the TP of prey µzoo and mesoZ remains unknown, and thus we estimate possible ranges of DF, using a range of TP. The following equations simplify the sum of terms to average TP for all µzoo and mesoZ prey:

$$TP_{GluMESO} = 1 * DF_{phyto+\mu zoo} + \overline{TP_{Glu_{mesoZ}}} * DF_{mesoZ} + 1 \quad (5)$$

$$TP_{AlaMESO} = 1 * DF_{phyto} + \overline{TP_{Ala_{\mu zoo}}} * DF_{\mu zoo} + \overline{TP_{Ala_{mesoZ}}} * DF_{mesoZ} + 1 \quad (6)$$

where MESO = mesozooplankton consumers, mesoZ = mesozooplankton prey, and µzoo = microzooplankton prey. We can re-arrange these equations to obtain DFs of mesoZ and µzoo in consumer diet as:

$$DF_{mesoZ} = \frac{TP_{GluMESO} - 2}{\overline{TP_{Glu_{mesoZ}}} - 1} \quad (7)$$

$$DF_{\mu zoo} = \frac{TP_{AlaMESO} - 2 - (TP_{Glu_{mesoZ}} - 1) * DF_{mesoZ}}{\overline{TP_{Ala_{\mu zoo}}} - 1} \quad (8)$$

For these, we assume that $TP_{AlamesoZ} = TP_{GlumesoZ} = 2$ (i.e. the mesozooplankton at the bottom of the food chain are herbivorous). This assumption is realistic and decreases the number of unknown variables so we can calculate different combinations of TP and DF for microzooplankton from the measurements made. However, this exercise is simply to show the possible range of microzooplankton dietary fractions.

Statistical analyses were done using MATLAB R2017b for TP calculations, estimations of statistical differences between In and Out groups, and for propagation of machine analytical error. The error for the TP calculations was done following standard error propagation rules, assuming TEF and β are constants, as (σ_{Phe}+ σ_{Tr})/TEF. Statistical tests for significance were done using non-parametric Kruskal-Wallis ANOVAs with a p-value of 0.05.

3. RESULTS

3.1. Phytoplankton, microzooplankton and mesozooplankton dynamics inside and outside of Opal

We briefly summarize production, growth and grazing rates from previous studies on Opal, which are important in understanding the biological effects of the eddy perturbation; detailed experimental results are presented elsewhere (e.g. Brown et al. 2008, Landry et al. 2008a,b). The cyclonic eddy Opal was mature and >1 mo old by the time it was first sampled. Phytoplankton production was initially high, ~1500 mg C m^{-2} d^{-1}, but the 5 d period of Opal growth-grazing experiments coincided with the late-bloom decline in which biomass crashed and euphotic zone productivity declined 3–4-fold to ambient levels (Fig. 3). Vertically integrated rates of grazing followed a similar trend, with microzooplankton grazing initially ~3-fold higher than ambient rates but approaching similar values to outside the eddy over the sampling period. Mesozooplankton grazing rates were generally lower than microzooplankton, but were also enhanced inside Opal and decreased over the sampling period. In contrast to microzooplankton grazing, however, mesozooplankton consumption of phytoplankton remained significantly higher within the eddy relative to waters outside Opal, despite the decreasing trend (Fig. 3). Mesozooplankton abundances were also higher at In stations, with some taxa higher inside of the eddy, including Clausocalanidae, *Eucalanus,* Poecilostomids (including *Oncaea*), Lucicutiidae and Mecynoceridae (Fig. 4).

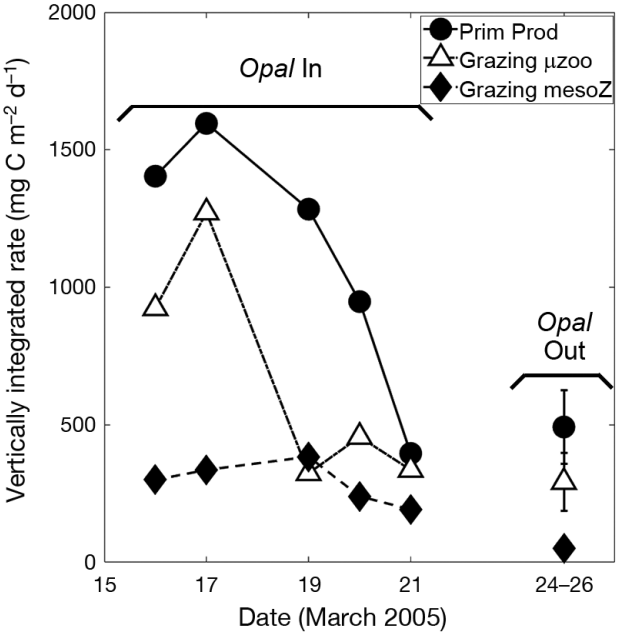

Fig. 3. Summary of vertically integrated production and grazing rates inside (In) and outside (Out) of cyclonic eddy Opal, showing primary production, microzooplankton (µzoo) grazing and mesozooplankton (mesoZ) grazing rates (mg C m^{-2} d^{-1})

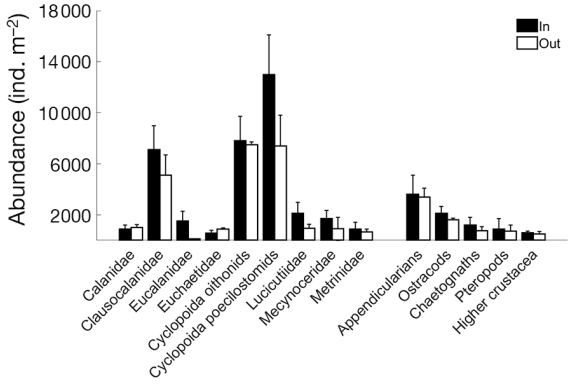

Fig. 4. Abundances of major zooplankton taxa collected at stations inside (In; black bars) and outside (Out; white bars) of cyclonic eddy Opal. Error bars are SD

3.2. Zooplankton TPs, TP_{Glu} and TP_{Ala}

The analyzed zooplankton taxa are organized according to increasing estimates of TP_{Glu} in Fig. 5, which roughly separates them into particle grazers (*Eucalanus* sp. adults, appendicularians, *Oithona*, *Eucalanus* spp. cop. and *Mecynocera clausii*) and carnivorous predators (*Pleuromamma* spp., *Lucicutia flavicornis*, *Stylocheiron carinatum* and *Euchaeta rimana*). *Oncaea* sp. falls at an intermediate TP relative to these 2 categories, reflecting its very different particle-associated lifestyle (Ohtsuka et al. 1996, Green & Dagg 1997, Steinberg et al. 1997) (Fig. 5a). The positions of copepods in the metazoan (TP_{Glu}) food web ranged between 2.0 and 3.2, for species assayed both inside and outside of the eddy (Fig. 5a).

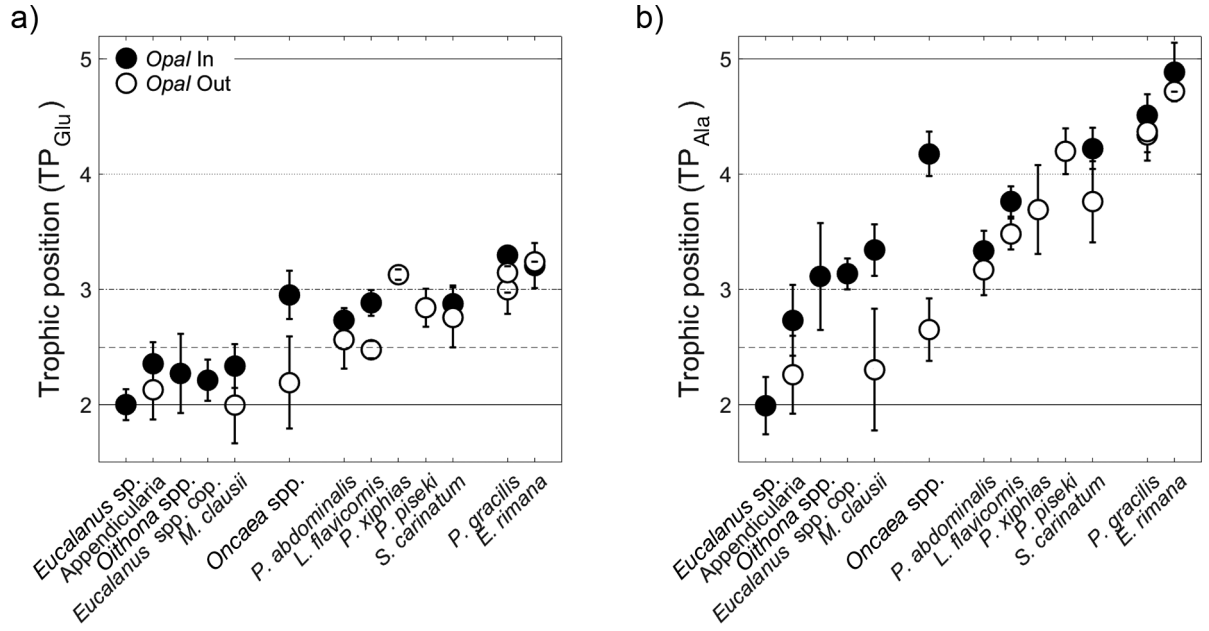

Fig. 5. Trophic positions (TPs) of assayed mesozooplankton taxa collected inside and outside of cyclonic eddy Opal. (a) TP_{Glu} is based on the $\delta^{15}N$ difference between glutamic acid and phenylalanine, and reflects steps within the metazoan (multicellular, mostly mesozooplankton) food web. (b) TP_{Ala} is based on the $\delta^{15}N$ difference between alanine and phenylalanine, which includes all steps (metazoan and protistan) including both meso- and micro-zooplankton. Error bars are SD

The range of TP_{Ala} was much higher, varying between 2.0 and 4.9 for individual taxa, reflecting their differences with respect to additional trophic transfers through protistan consumers (Fig. 5b). *Eucalanus* sp. adults were the only entirely herbivorous zooplankton among the groups analyzed, with TP_{Glu} = TP_{Ala} = 2.0 (Fig. 5, Table S2). All other taxa showed significant differences between TP_{Glu} and TP_{Ala} (Kruskal-Wallis, $p < 0.05$). *Eucalanus* spp. cop. had a slightly higher TP_{Glu} = 2.2, and a much higher TP_{Ala} = 3.1 (Fig. 5) compared to adults. Both *Eucalanus* adults and copepodites were only assayed inside of the eddy, because they were extremely rare in the collections outside.

Appendicularians outside of the eddy had similar TPs based on Glu and Ala (2.1/2.3 respectively, Fig. 5), but TPs were more different in the eddy. *Oithona* sp. was only assayed from inside the eddy, where the high ΔTP = 0.8 (Fig. 6; TP_{Glu} = 2.3 ± 0.3 [SD]; TP_{Ala} = 3.1 ± 0.5) indicates the substantial contribution of heterotrophic protists to its diet. *M. clausii* showed substantial variability in TP_{Glu} and TP_{Ala} between sampling locations (Figs. 5 & 6), suggesting differences in the underlying food webs. The contribution of protists to *M. clausii* diet inside of the eddy was enhanced compared to appendicularians, which had a similar TP_{Glu} (~2.0), and also enhanced compared to *P. abdominalis*, which had higher TP_{Glu} (~2.5) than *M. clausii*. These differences between

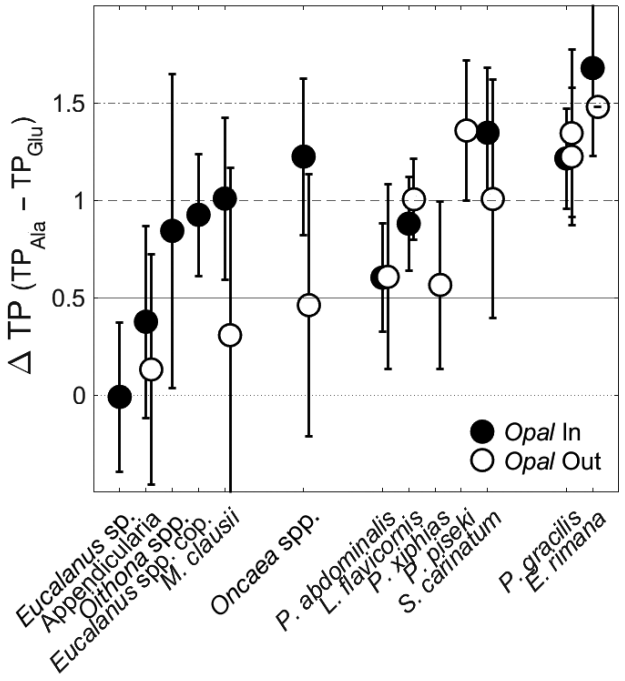

Fig. 6. Difference between the 2 trophic indices (ΔTP = TP_{Ala} – TP_{Glu}; see Fig. 5 for definitions) reflects the integrated protistan contribution to the absolute trophic level of each species. Filled circles are for specimens collected inside ('In'), open circles represent specimens collected outside ('Out') of cyclonic eddy Opal. Error bars are SD ($\sigma_{\Delta TP} = \sigma_{TPGlu} + \sigma_{TPAla}$)

food webs are further supported by the ΔTP of *Oncaea* sp., with the largest difference in both TP_{Glu} and TP_{Ala} between sampling locations (Fig. 5). Inside the eddy, a full protistan trophic step separated *Oncaea* and the microzooplankton, but the ΔTP was only 0.5 outside of the eddy (Fig. 6).

We were able to assay 2 *Pleuromamma* species outside and inside of the eddy. *P. abdominalis* gave TP_{Glu} = 2.6 /2.7 (Out/In), and TP_{Ala} = 3.2/3.3, while *P. gracilis* had TP_{Glu} = 3.0/3.3, and TP_{Ala} = 4.3/4.5. Two other species, *P. xiphias* and *P. piseki* had TP_{Glu} = 3.1 and 2.8, and TP_{Ala} = 3.7 and 4.2, respectively, and were only sampled outside of the eddy. The ΔTP for all *Pleuromamma* species varied between 0.5 and 1.4 TP, with *P. piseki* and *P. gracilis* on the higher end. Finally, for both Out/In, *E. rimana* had the highest TP_{Glu} (3.2/3.2) and TP_{Ala} (4.7/4.9) of the assemblage, and these differed by about 1.5 TP (Figs. 5 & 6; Table S2).

3.3. Changes in TP inside the eddy

TPs were either consistently higher inside the eddy or not different between locations, such that no significant differences were found when all groups were tested together (Fig. 7, Kruskal-Wallis, $p > 0.05$). However, differences among particle-grazing mesozooplankton, TP_{Glu} <2.5, were significant (Kruskal-Wallis, $p < 0.05$), suggesting generally enhanced contributions of heterotrophic protists to the omnivorous mesozooplankton in Opal. Appendicularia, *M. clausii* and *Oncaea* spp. all had higher TP_{Ala} inside the eddy, and some of these TPs were comparable to the more predatory taxa (*Pleuromamma* spp., *L. flavicornis* and *S. carinatum*; Fig. 5b).

For the 8 taxa that could be compared, *Oncaea* spp. showed the greatest In–Out TP difference, with TP_{Ala} increasing 1.5 ± 0.2 and TP_{Glu} increasing 0.8 ± 0.3, indicating proportional lengthening of both the protistan and metazoan components of the plankton food web. *M. clausii* followed *Oncaea* spp. in trophic variability, with TP_{Glu} and TP_{Ala} enhanced 0.3 ± 0.2 and 1.0 ± 0.4, respectively, inside Opal, suggesting a disproportionate eddy enhancement of food-web pathways through heterotrophic protists. TP changes were less pronounced for appendicularians and *S. carinatum* (change in TP_{Ala} = 0.5/0.5; change in TP_{Glu} = 0.2/0.1, respectively). *L. flavicornis* showed similar changes in TP_{Glu} and TP_{Ala} (0.4 ± 0.1 and 0.3 ± 0.1, respectively), suggesting an enhanced reliance on metazoan prey inside the eddy. Finally, for *P. abdominalis*, *P. gracilis* and *E. rimana*, the In–Out TP differences were slightly positive but not significantly different from 0 (Fig. 7).

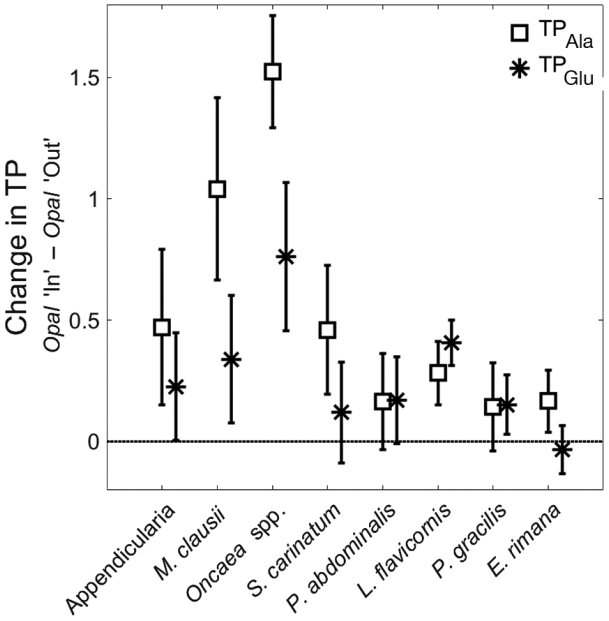

Fig. 7. Change in trophic positions (TPs) for mesozooplankton taxa sampled inside (In) and outside (Out) of cyclonic eddy Opal. Changes in TP_{Ala} are represented by squares, and changes in TP_{Glu} are represented by asterisks. Error bars are SD

3.4. Shifts in the nitrogen baseline (Phe and source AAs)

Changes in the average $\delta^{15}N$ values of all zooplankton AAs are presented in Fig. 8. The source AAs Gly, Lys and Thr showed higher $\delta^{15}N$ inside Opal, but only the increase for Thr was significant (Kruskal-Wallis, $p < 0.05$).

Looking more closely at Phe, the canonical source AA (Chikaraishi et al. 2009, Hannides et al. 2009, Nielsen et al. 2015, Mompeán et al. 2016, Ohkouchi et al. 2017), we found a large range (~9‰) in Phe $\delta^{15}N$ values for all zooplankton taxa both inside and outside of Opal, but both maximum and minimum values were in the eddy. *Eucalanus* sp. adults (Phe $\delta^{15}N$ = 3.3 ± 0.6‰) had the highest Phe values, and along with *Eucalanus* spp. cop. (Phe $\delta^{15}N$ = 2.0 ± 0.5‰) showed their highest values inside the eddy (Fig. 9a). In contrast, Phe values for *Oncaea* spp. (Phe $\delta^{15}N$ = –4.9 ± 0.6‰) and *L. flavicornis* (Phe $\delta^{15}N$ = –3.3 ± 0.5‰) were lowest overall, but only for specimens sampled inside the eddy, while their values were closer to average outside of Opal. In general, Phe values outside of the eddy were less variable, with *P. ab-*

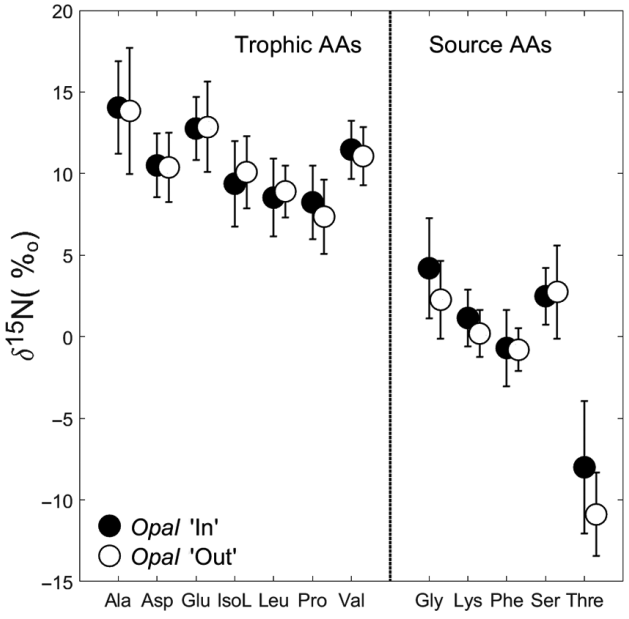

Fig. 8. Mean (±SD) amino acid $\delta^{15}N$ values of all zooplankton sampled. Filled circles represent samples from inside (In) cyclonic eddy Opal, open circles are zooplankton sampled outside (Out) of Opal

dominalis (Phe $\delta^{15}N = 1.7 \pm 0.7$‰) being the highest of the sampled taxa, followed by *M. clausii* (Phe $\delta^{15}N = 0.7 \pm 0.9$‰). *P. piseki* gave the lowest Phe $\delta^{15}N$ value of -2.85 ± 0.3‰ outside of the eddy, and the remaining taxa had values of 0 to −2.0‰ (Fig. 9a).

For the taxa that can be compared, Phe $\delta^{15}N$ values generally decreased in Opal, with the exception of appendicularians and *S. carinatum*, for which changes were not significantly different from 0 (Fig. 9b). *Oncaea* spp. and *L. flavicornis* showed the greatest Phe depletions (-2.7 ± 0.7‰), followed by *M. clausii*, *P. abdominalis*, *P. gracilis* and *E. rimana* (Fig. 9b).

4. DISCUSSION

We hypothesized that the enhanced diatom biomass and productivity inside of Opal (Brown et al. 2008, Landry et al. 2008a, McAndrew et al. 2008) would produce a shorter, more direct food-web pathway to mesozooplankton. This is consistent with conventional thinking that associates large phytoplankton with eutrophy and higher grazing by mesozooplankton within a 'classical food chain,' and small phytoplankton with oligotrophy and high grazing by microzooplankton within a 'multivorous food web' (Fig. 1, e.g. Legendre & Rassoulzadegan 1995). While this may reasonably describe trophic variability on large scales, we found the opposite result for the perturbed eddy system. According to CSIA-AA, zooplankton TPs inside the eddy were either similar or higher than in the adjacent environment, especially for TP_{Ala} of groups closer to the food-web base (Figs. 5b & 7).

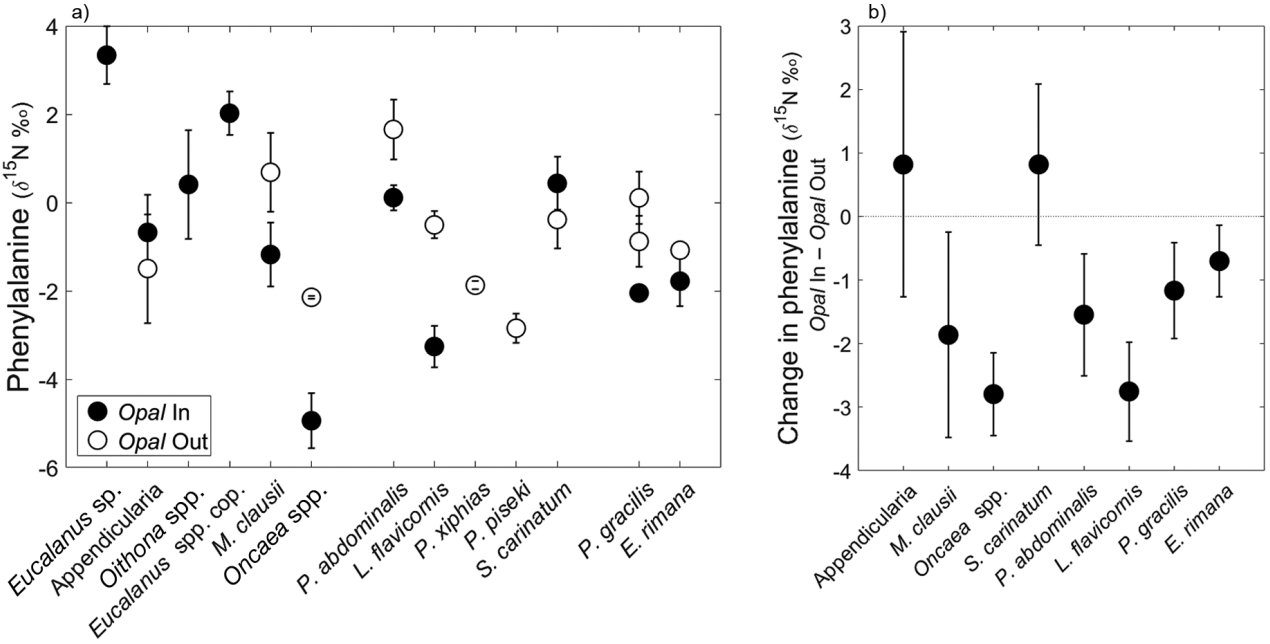

Fig. 9. (a) $\delta^{15}N$ of phenylalanine (Phe) for all analyzed mesozooplankton taxa. Filled (open) circles indicate organisms sampled inside (outside) of cyclonic eddy Opal. Error bars are standard deviations of 3 machine runs. (b) Difference in Phe $\delta^{15}N$ in animals collected inside and outside of Opal

The isotopic analyses also showed differences in source N and trophic enrichment of individual taxa that provide new insights on aspects of their trophic ecologies, including the likely role of detrital feeding and potential niche separation of 4 co-occurring species of the genus *Pleuromamma*. In the sections below, we consider these results in the context of what is known about the dynamics of biomass, productivity and grazing in the eddy.

4.1. Temporal scales of variability in food-web perturbation response

The magnitudes of the physical and biological perturbations associated with Opal were on the extreme end for mesoscale eddies that have been studied to date in the subtropical Pacific (Seki et al. 2001, Bidigare et al. 2003, Vaillancourt et al. 2003, Brown et al. 2008, Rii et al. 2008), providing an important opportunity to quantify food web responses to a substantial and lingering event. When Opal was first sampled in mid-March 2005, it had been visible for about 1 mo in MODIS SST imagery, and it remained trackable for an additional month (Dickey et al. 2008, Nencioli et al. 2008). However, the experimental time frame corresponded to the late-bloom period when the phytoplankton community crashed (Fig. 3, Landry et al. 2008a), showing strong temporal variability during the period of our sampling.

Three distinct layers within the Opal water column could be identified, based on plankton rates and standing stocks. Biomass and composition of the phytoplankton community was similar to waters outside of the eddy in the upper mixed layer (0–40 m), but rates of growth and grazing were enhanced. Distinct differences in biomass and composition were found in the deep layer (70–90 m), with a large increase in >20 µm diatoms (~100-fold greater than in waters outside of the eddy). The 50–60 m layer between the surface and deep waters was characterized by elevated biomass of senescent diatoms, and enhanced grazing with respect to production, as their growth rates were depressed in this layer (Brown et al. 2008, Landry et al. 2008a). This vertical habitat structuring likely had an effect on food-web structure and the baseline nitrogen of phytoplankton, which could help explain the high variability in the source AA Phe of different zooplankton taxa (Fig. 9).

One likely explanation for the disparity between the zooplankton TP estimates from CSIA-AA (suggesting enhanced mesozooplankton omnivory in the eddy) and the fluxes from production-grazing experiments (suggesting enhanced mesozooplankton herbivory inside Opal) is that they apply to different time periods in the eddy's life cycle. Isotopic signatures accumulate in copepod tissue based on dietary intake and metabolism over the course of development and somatic growth from nauplius to adult. If adult female copepods, such as we sampled for CSIA-AA, pass most of their daily diet to egg production, the isotopic compositions of their body tissues could have been set, possibly weeks prior, under environmental conditions during the early phase of the eddy bloom. The observed dynamics of the mixed layer stratum in Opal illustrates how nutrient inputs can stimulate productivity of the ambient picophytoplankton community with little effect on phytoplankton biomass but substantially increasing grazing, productivity and biomass of microzooplankton, especially large ciliates (Landry et al. 2008a). Such a scenario, if generalized to an earlier state of the bloom, could support both a higher rate of microzooplankton prey availability and a longer (picoplankton–nanoflagellate–ciliate) food chain to mesozooplankton.

The importance of the time element in interpreting the trophic data can also be seen in the isotope enrichment differences of carnivorous versus suspension-feeding taxa (Fig. 5). The fact that carnivorous taxa (e.g. *Euchaeta rimama* and *Pleuromamma gracilis*) show modest to little change in trophic isotopic enrichment compared to taxa closer to the base of the food web indicates that considerable time is required for the signal to propagate through the trophic hierarchy because each level must gradually alter its isotopic composition in response to dietary changes before it can influence the next level. We thus interpret the isotopic evidence for elevated TPs of suspension-feeding zooplankton in Opal as providing a unique perspective on the early response (i.e. predating our direct experimental observations) of an oligotrophic open-ocean food web to a major nutrient input perturbation.

Using *Oncaea* spp., a strongly aggregate-associated copepod genus (Steinberg et al. 1994, Ohtsuka et al. 1996, Green & Dagg 1997), as an indicator organism, CSIA-AA also suggests a potentially important role of detritus feeding in explaining the elevated TP response to Opal's diatom bloom. *Oncaea* spp. showed by far the largest TP change (1.5 steps for TP_{Ala}; Figs. 5 & 6; Table S2) of all taxa analyzed, with TP estimates similar to suspension feeders (i.e. *Eucalanus*, appendicularians, *Oithona* and *M. clausii*, Fig. 5) outside of the eddy, but with higher TPs, comparable to carnivorous taxa, inside of the eddy. This result

suggests that aggregates were local sites of elevated microbial food-web activity and isotopic enrichment. Consistent with this ΔTP of *Oncaea* spp., other studies have indicated elevated rates of remineralization in the 100–150 m depth within the eddy, based on ^{234}Th (Maiti et al. 2008), and δ^{15}N of particulate nitrogen (Mahaffey et al. 2008). Enhanced δ^{15}N of particulate nitrogen could have resulted from the higher input of heavy nitrate sources, but re-working (alteration with respect to the baseline) of AAs by microzooplankton (Décima et al. 2017) or bacteria (Calleja et al. 2013) likely plays a role altering ^{15}N values, including those of source AAs. Detrital feeding could well be an important contributor to their observed isotopic enrichments in the eddy, assuming that all suspension-feeding taxa include at least some detritus in their diets (Steinberg et al. 1994, Möller et al. 2012).

Enhanced δ^{15}N in Gly, Lys and Thr follow the same pattern of particulate nitrogen (Fig. 8), although the pattern was only significant for Thr (Kruskal-Wallis, $p < 0.05$) where isotopic values were enhanced inside Opal at depths >50 m (Mahaffey et al. 2008). Some of this pattern may be related to enhanced delivery of nitrate, but remineralization cannot be ruled out. Calleja et al. (2013) found that Gly was highly and consistently altered, compared to the phytoplankton source material, through bacterial processes. Metabolism of Thr is complex, displaying both source and trophic characteristics and making the interpretation of shifts in its δ^{15}N difficult. It has thus been classified as a 'metabolic' AA, outside of source and trophic definitions (Germain et al. 2013). However, the degree of dissimilarity in Thr does suggest metabolic activity, potentially linked to microbial activity (Fig. 8). These multiple lines of evidence support the conclusion that remineralization and microbial activity were substantially elevated along with production in Opal, further rejecting our original hypothesis that nutrient injection into an oligotrophic system approximates the conditions and/or the food web of a eutrophic system.

While issues related to the CSIA-AA methodology could have contributed to our results, we consider their effects less likely than those described above. There is ample evidence that the TEFs used to estimate TPs can vary with TP (Hoen et al. 2014), diet (McMahon et al. 2015), laboratory versus field estimates (McClelland & Montoya 2002, Bradley et al. 2015) and type of organism (Lorrain et al. 2009, Dale et al. 2011, Gutiérrez-Rodríguez et al. 2014). For example, when fed a monoalgal herbivorous diet in controlled laboratory experiments, *Calanus pacificus* had higher TEFs (TEF_{Glu} = 7.6, TEF_{Ala} = 6.1) than on a diet of protistan microzooplankton (TEF_{Glu} ~ TEF_{Ala} ~ 5) (Décima et al. 2017). To reflect mixed diets and to be consistent with other recent studies (Bradley et al. 2015, Nielsen et al. 2015), we used intermediate and proportionally lower (1.5‰/1.2‰) values of TEF_{Glu} = 6.1 and TEF_{Ala} = 4.5 than those of Chikaraishi et al. (2009). If TEFs in the field were higher inside the eddy than outside, our resulting TP calculations would have been more similar for In and Out analyses. However, using higher TEFs inside the eddy would also have produced unrealistically low TP estimates (<2.0) for *Eucalanus* sp. Overall, while there is still a need to be cognizant of such effects, there is little specific evidence that points to TEF variability as a significant issue for interpreting results of the present study.

Additional methodological issues related to preservation deserve consideration as well. Samples had been preserved in formalin for 3 yr prior to sorting and analyses. Early studies have shown that the isotopic signatures of bulk nitrogen of zooplankton do not change appreciably, even after 2 (Mullin et al. 1984) to 11 yr (Rau et al. 2003) of formalin preservation, and this was subsequently confirmed for AA analyses (Hannides et al. 2009, Hetherington et al. 2019). All samples experienced similar times and conditions of preserved storage, sorting and isotope analyses. Because of this, we assume that these CSIA-AA results can at least be compared in a relative sense and do not bias our main conclusions.

4.2. Taxon-specific responses to the bloom perturbation

Zooplankton taxa displayed very different responses to the diatom bloom in *Opal. Oncaea* spp. and *Eucalanus* sp. were among the taxa whose abundances increased substantially, Eucalanidae, in particular, being 15 times more abundant inside the eddy than outside (Fig. 4). As previously noted, *Oncaea* spp. showed the strongest isotopic enrichment and TP change (+1.5) of all analyzed taxa, which presumably reflects their feeding on active microbial communities on particle aggregates. *Oncaea* spp. also had the lowest δ^{15}N values for Phe (–5‰), which would suggest an N source based strongly on recycling of light N (metabolic fractionation). In contrast, *Eucalanus* sp. had the lowest TP estimate (2.0), which is assumed to reflect its almost exclusive feeding on large diatoms in the lower euphotic zone (70–90 m). This is consistent with *Eucalanus* sp. having the

highest $\delta^{15}N$ value for Phe (+3.5‰), indicating that upwelled deep nitrate contributed more to the source N supporting the food web to this species than to others, and consistent with higher $\delta^{15}N$ of deep particulate nitrogen inside Opal (Mahaffey et al. 2008). As reported by Landry et al. (2008b), the adult *Eucalanus* analyzed in this study are believed to be *E. spinifer*, relatively large animals of the *E. hyalinus* group (Goetze 2005). The *Eucalanus* copepodites analyzed are more likely a mixture of co-dominants, including *Subeucalanus subtenuis* and *Subeucalanus subcrassus*. While the copepodites had high $\delta^{15}N$ Phe, similar to the *Eucalanus* adults, their mean TP was substantially higher, suggesting stronger, perhaps selective, feeding on protistan microzooplankton (TP_{Ala}).

Mecynocera clausii (cruising suspension-feeder) and appendicularians both had similar and intermediate values of TP_{Glu} (<2.4) and $\delta^{15}N$ Phe compared to *Oncaea* spp. and *Eucalanus* sp. Neither showed much of a change in source N in the eddy, with appendicularians increasing slightly and *M. clausii* decreasing in the eddy to almost the same $\delta^{15}N$ Phe. This suggests to us that their population centers were most likely in the upper mixed layer where the observed eddy simulation effects were primarily an increase in the turnover rate of the ambient phytoplankton community (increased coupled production, grazing and remineralization) and enhanced productivity and biomass of protistan microzooplankton. *M. clausii* did, in fact, display a strong TP_{Ala} increase in the eddy, consistent with a disproportionate dietary input of microzooplankton. Appendicularians showed much less of a TP_{Ala} increase, which likely results from a feeding apparatus optimized for consuming very small particles, from a few microns to submicron-sized particles (Flood et al. 1992, Flood & Deibel 1998), allowing larger microzooplankton, like ciliates, to evade being entrained and captured on their mucus houses. Active capture by copepods, in contrast, would allow more efficient consumption of larger microzooplankton. In this regard, *Oithona* spp., small ambush predators of microzooplankton, had isotopic characteristics also identical to *M. clausii* inside Opal. On this basis, we would also put *Oithona* spp. as mainly in the mixed layer stratum, although we have no comparative isotopic measurements for that taxon outside of Opal.

As previously indicated, the more carnivorous species that we examined probably had insufficient time in the eddy to come into isotopic equilibrium with their prey. Migratory species like *Pleuromamma* may also have moved in and out of the eddy as it was being advected southward (Nencioli et al. 2008), although the changes in their isotopic values in and out of the eddy are similar to what we observed for the carnivorous non-migrating copepod *Euchaeta rimana*. While these factors make the magnitudes of isotopic changes difficult to interpret for higher-level consumers, it is clear that their trends are at least similar to those of taxa closer to the base of the food web.

4.3. Implications for trophic niche separation of *Pleuromamma* species

Co-occurring species of the strongly migrating genus *Pleuromamma* have been used in previous investigations of how congeners may partition the open-ocean environment so as not to compete directly. For our study region in the subtropical North Pacific, Ambler & Miller (1987) found that modal day- and nighttime vertical distributions differed among 3 species, with females of *P. gracilis* occupying shallower depth strata (300 m day, 25 m night), *P. xiphias* occupying deeper strata (>400 m day, 100 m night) and *P. abdominalis* occurring at intermediate depths (100 m deeper than *P. gracilis* during the day, 50–75 m at night, Table 2). Haury (1988) found broader distributional overlap among species in the eastern Pacific, but his few samples (3 daytime, 1 nighttime) of finely resolved distributions from the NPSG are generally consistent with the conclusions of Ambler & Miller (1987) and provide additional

Table 2. Mean depths of occurrence, phenylalanine (Phe ‰) and trophic positions using glutamine or alanine as the trophic amino acid to estimate trophic transfers (TP_{Glu} and TP_{Ala}, respectively) for 4 *Pleuromamma* species sampled outside of Opal. For *P. gracilis*, we ran 2 sets of samples (replicates 1 and 2), which show the natural ecological and baseline variability within 1 species. Estimates of day and night residence depths are from Ambler & Miller (1987) and Hayward (1980)

Species	Residence depth (m) Night	Day	Phe (‰)	TP_{Glu}	TP_{Ala}
P. gracilis 1	25–75	300	0.1 ± 0.6	3.0 ± 0.2	4.3 ± 0.2
P. gracilis 2	25–75	300	−0.9 ± 0.6	3.1 ± 0.2	4.4 ± 0.2
P. abdominalis	50–75	400	1.7 ± 0.7	2.6 ± 0.2	3.2 ± 0.2
P. piseki	0–170	300	−2.9 ± 0.3	2.8 ± 0.2	4.2 ± 0.2
P. xiphias	50–200	>400	−1.9 ± 0.1	3.1 ± 0.04	3.7 ± 0.4

information on *P. piseki*, which overlaps with *P. gracilis* during the daytime but is more uniformly distributed throughout the euphotic zone (upper 170 m) at night than any of the other species (Table 2). Despite these apparent distributional differences, Hayward (1980) observed that feeding indices, measured as relative gut fullness, covaried positively among all species for all scales of spatial and temporal variability, failing to reveal the circumstances where individual species might have an advantage over the others. We therefore asked here whether differences in source N and trophic AA enrichment from CSIA-AA might provide new insights into possible trophic differences that set these species apart.

According to our results for *Pleuromamma* species outside of the eddy (where we sampled all 4 species), *P. gracilis* had source and trophic AA characteristics that were most like those of *E. rimana*, a known carnivore in the upper euphotic zone (Ambler & Miller 1987). TP_{Glu} values of both are slightly greater than 3.0, a signature of direct predation on other metazoans. In addition, their TP_{Ala} values both point to food-web pathways with an additional >1 trophic transfer steps through protistan microzooplankton (Fig. 5; Table S2). At the other end of the trophic spectrum for *Pleuromamma* species, *P. abdominalis* shows a TP_{Glu} that is 0.5 less than *P. gracilis*, and a full trophic level less in TP_{Ala}. This indicates a diet that has a greater phytoplankton contribution compared to *P. gracilis* (i.e. more omnivorous). In addition, their nighttime distributions coupled with the higher $\delta^{15}N$ Phe of *P. abdominalis* and *P. gracilis* suggest that both of these species feed in a similar, shallower stratum, with ^{15}N of particulate organic matter (POM) particles suggesting depths of 20–50 m (Mahaffey et al. 2008).

The 2 remaining species are deeper dwelling, and their depleted Phe values suggest they feed at depths between 50 and 100 m (Table 2), assuming the baseline Phe ^{15}N follows the same pattern as bulk POM (Mahaffey et al. 2008), albeit with lower isotopic content (Hannides et al. 2013). *P. piseki* appears to have dietary characteristics similar to *P. gracilis*, with strong feeding on both metazoan and protistan microzooplankton prey. *P. xiphias*, the deepest-living species, also exhibits comparably high carnivorous feeding on metazoan prey ($TP_{Glu} \geq 3$) as *P. gracilis* and *E. rimana*, but exploits a food web with 0.7–0.8 fewer trophic steps ($TP_{Ala} - TP_{Glu} = 0.5$ versus 1.2–1.3) through protistan consumers, although consumption of detritus cannot be discounted. Such conditions might exist, for example, for small metazoans that feed primarily on phytoplankton in the deep chlorophyll maximum, which in stations outside of the eddy coincided with depleted $\delta^{15}N$ bulk POM values at depths of 80 and 120 m (Mahaffey et al. 2008).

While these speculations about possible feeding niche differences among co-occurring *Pleuromamma* species would need to be confirmed in a more detailed and focused study, perhaps done in conjunction with molecular analyses of gut contents, they illustrate that substantial variability exists among similar species and the underlying food webs in the open ocean, and the potential of isotopic approaches to interpreting these differences.

4.4. Plankton community variability and resiliency in the NPSG

In a multi-year study of zooplankton collected at Station ALOHA, Hannides et al. (2009) found notable seasonal variability in the baseline N, a 6‰ range in Phe $\delta^{15}N$ values indicative of a system shift from nitrate-based productivity in winter to diazotrophy-based production in summer, although the calculated TPs (TP_{Glu}) of individual species remained relatively constant overall. The diatom bloom perturbation in Opal was a much stronger test of the system's ability to restructure and capitalize on a major productivity event. Interestingly, while we did observe enhanced grazing by mesozooplankton on phytoplankton, at least during the late bloom phase, this did not result in a weakening of the trophic link between microzooplankton and mesozooplankton.

Enhanced TP_{Ala} of particle-feeding zooplankton (Figs. 5b & 6) suggests that mesozooplankton consumption of microzooplankton increased disproportionally in the eddy or that the microzooplankton food chain was lengthened. While these 2 alternatives or combinations thereof cannot be distinguished with the available data, Eqs. (7) and (8) can be used to determine different combinations of mean microzooplankton $TP_{\mu zoo}$ (TP) and $DF_{\mu zoo}$ (dietary fraction or fractional contribution of microzooplankton to mesozooplankton diet) that are consistent with the data. Using *Eucalanus* copepodites ('In', TP_{Ala} = 3.1, TP_{Glu} = 2.2) as an example of particle-feeding mesozooplankton (Fig. 5), Eq. (7) with TP_{Glu} = 2.2 indicates that metazoan prey comprise 20% (0.2) of dietary N while the combination of phyto- and microzooplankton accounts for the remaining 80% (0.8). Inserting these results into Eq. (8) leads to TP_{Ala} = 3.1 ± 0.5 (Fig. 5b), with the error from the standard deviation of TP_{Ala} (Fig. 10). The values of 2.0, 2.5, 3.0 and 3.5 for $TP_{\mu zoo}$ imply microzooplankton proportional

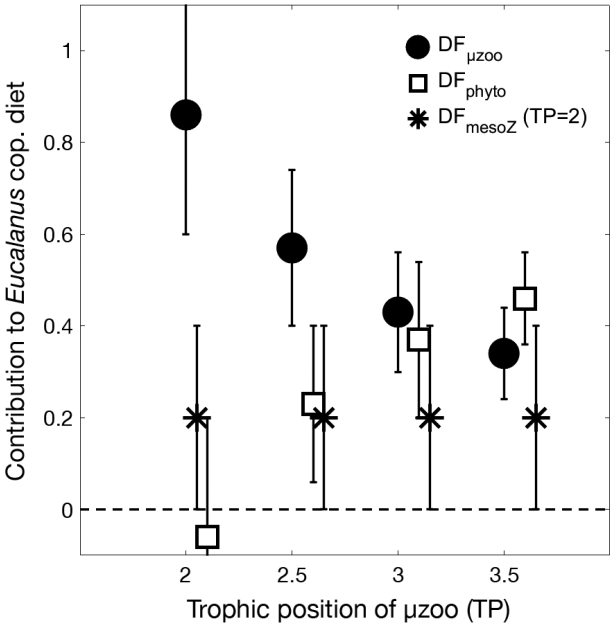

Fig. 10. Estimates of the dietary fractional contributions of microzooplankton ($DF_{\mu zoo}$, black circles), phytoplankton (DF_{phyto}, white squares) and mesozooplankton (DF_{mesoZ}, asterisks) to *Eucalanus* copepodites, as a function of possible trophic position of microzooplankton. Error bars are SD

contributions of 0.86, 0.57, 0.43 and 0.34, respectively, to the diets of *Eucalanus* cop. (Fig. 10). An interesting conclusion from this exercise is that it was unlikely that any microzooplankton with TP = 2 were being consumed by *Eucalanus* cop. (or other suspension-feeding mesozooplankton by implication), since this would not indicate any consumption of phytoplankton (Fig. 10). Direct consumption of phytoplankton by *Eucalanus* is supported by the TP of adult specimens (TP = 2), their high abundance in the eddy (Fig. 9) and measurements of enhanced grazing by the mesozooplankton community (Landry et al. 2008b), which supports additional trophic steps in the microzooplankton food web. Using the measured CSIA-AA values and assuming an average microzooplankton TP of 3.0 (assuming 1 flagellate to ciliate step, Landry et al. 2008b), metazoan prey contributed 0.2, protistan microzooplankton 0.43, and phytoplankton 0.37 to the diet of a particle-feeding zooplankter within the eddy (copepodites, in this case). However, while this is a likely scenario, there is a range of possible combinations with these measurements (Fig. 10). The mean TP of microzooplankton is clearly important in determining these dietary percentages, as the phytoplankton contribution decreases proportionally with increasing $TP_{\mu zoo}$.

In general, our CSIA-AA results for multiple species suggest a disproportionate time-averaged increase in N flow-through microbial processes relative to direct feeding on phytoplankton. A strongly stimulated microbial food web was the primary eddy effect on the mixed-layer community, and even the microzooplankton grazing impact on large diatoms inside Opal (58% of their production) was similar to microzooplankton grazing on the ambient phytoplankton community (59% of production) outside of the eddy (Landry et al. 2008a). This suggests that while plankton systems can be characterized based on their rates of nutrient supply (e.g. Legendre & Rassoulzadegan 1995), short-term changes in nutrient inputs do not necessarily alter the dominant trophic pathways in a dramatic fashion. Similarly, Calbet & Landry (2004) observed surprisingly little difference among open-ocean to coastal and tropical to polar ecosystems in terms of the mean proportions of phytoplankton productivity consumed by microzooplankton. Rapid growth rates and trophic flexibility of protistan microzooplankton apparently allow the microbial community to reorganize quickly to bloom perturbations such that this portion of the food web is relatively resilient to change.

Acknowledgements. We gratefully acknowledge the assistance of Melinda Simmons with shipboard sampling, Kate Tsyrklevich with zooplankton sorting, and Ann Townsend and Linsey Sala of the SIO Pelagic Invertebrates Collections with species identification. We thank Elizabeth Gier and Brian Popp for help with CSIA-AA analyses. We also thank Lujan Décima for the original copepod illustrations. We are indebted to 3 anonymous reviewers for comments that have greatly improved this manuscript. This study was supported by NIWA COES1901 and COES2001 to M.D., and by U.S. National Science Foundation grants OCE-0324666, -1260055 and -1756517 to M.R.L. CSIA-AA data are available through the Biological and Chemical Oceanography Data Management Office under the project title 'CSIA-AA Mesozooplankton TP' (www.bco-dmo.org/project/556514).

LITERATURE CITED

Ambler JW, Miller CB (1987) Vertical habitat partitioning by copepodites and adults of subtropical oceanic copepods. Mar Biol 94:561–577

Benitez-Nelson CR, McGillicuddy DJ (2008) Mesoscale physical-biological-biogeochemical linkages in the open ocean: an introduction to the results of the E-Flux and EDDIES programs — Preface. Deep Sea Res II 55: 1133–1138

Benitez-Nelson CR, Bidigare RR, Dickey TD, Landry MR and others (2007) Mesoscale eddies drive increased silica export in the subtropical Pacific Ocean. Science 316: 1017–1021

Bidigare RR, Benitez-Nelson C, Leonard CL, Quay PD, Parsons ML, Foley DG, Seki MP (2003) Influence of a

cyclonic eddy on microheterotroph biomass and carbon export in the lee of Hawaii. Geophys Res Lett 30:1318

Bradley CJ, Wallsgrove NJ, Choy CA, Drazen JC, Hetherington ED, Hoen DK, Popp BN (2015) Trophic position estimates of marine teleosts using amino acid compound specific isotopic analysis. Limnol Oceanogr Methods 13: 476–493

Brown SL, Landry MR, Selph KE, Jin Yang E, Rii YM, Bidigare RR (2008) Diatoms in the desert: plankton community response to a mesoscale eddy in the subtropical North Pacific. Deep Sea Res II 55:1321–1333

Calbet A (2008) The trophic roles of microzooplankton in marine systems. ICES J Mar Sci 65:325–331

Calbet A, Landry MR (1999) Mesozooplankton influences on the microbial food web: direct and indirect trophic interactions in the oligotrophic open ocean. Limnol Oceanogr 44:1370–1380

Calbet A, Landry MR (2004) Phytoplankton growth, microzooplankton grazing, and carbon cycling in marine systems. Limnol Oceanogr 49:51–57

Calbet A, Saiz E (2005) The ciliate-copepod link in marine ecosystems. Aquat Microb Ecol 38:157–167

Calleja ML, Batista F, Peacock M, Kudela R, McCarthy MD (2013) Changes in compound specific $\delta^{15}N$ amino acid signatures and D/L ratios in marine dissolved organic matter induced by heterotrophic bacterial reworking. Mar Chem 149:32–44

Chenillat F, Franks PJS, Riviere P, Capet X, Grima N, Blanke B (2015) Plankton dynamics in a cyclonic eddy in the Southern California Current System. J Geophys Res Oceans 120:5566–5588

Chikaraishi Y, Ogawa NO, Kashiyama Y, Takano Y and others (2009) Determination of aquatic food-web structure based on compound-specific nitrogen isotopic composition of amino acids. Limnol Oceanogr Methods 7: 740–750

Dale JJ, Wallsgrove NJ, Popp BN, Holland KN (2011) Nursery habitat use and foraging ecology of the brown stingray *Dasyatis lata* determined from stomach contents, bulk and amino acid stable isotopes. Mar Ecol Prog Ser 433:221–236

Décima M, Landry MR, Popp BN (2013) Environmental perturbation effects on baseline $\delta^{15}N$ values and zooplankton trophic flexibility in the southern California Current Ecosystem. Limnol Oceanogr 58:624–634

Décima M, Landry MR, Bradley CJ, Fogel ML (2017) Alanine $\delta^{15}N$ trophic fractionation in heterotrophic protists. Limnol Oceanogr 62:2308–2322

Dickey TD, Nencioli F, Kuwahara VS, Leonard C and others (2008) Physical and bio-optical observations of oceanic cyclones west of the island of Hawai'i. Deep Sea Res II 55:1195–1217

Falkowski PG, Ziemann D, Kolber Z, Bienfang PK (1991) Role of eddy pumping in enhancing primary production in the ocean. Nature 352:55–58

Flood PR, Deibel D (1998) The appendicularian house. In: Bone Q (ed) The biology of pelagic tunicates. Oxford University Press, New York, NY, p 105–124

Flood PR, Deibel D, Morris CC (1992) Filtration of colloidal melanin from seawater by planktonic tunicates. Nature 355:630–632

Germain LR, Koch PL, Harvey J, McCarthy MD (2013) Nitrogen isotope fractionation in amino acids from harbor seals: implications for compound-specific trophic position calculations. Mar Ecol Prog Ser 482:265–277

Goetze E (2005) Global population genetic structure and biogeography of the oceanic copepods *Eucalanus hyalinus* and *E. spinifer*. Evolution 59:2378–2398

Goldthwait SA, Steinberg DK (2008) Elevated biomass of mesozooplankton and enhanced fecal pellet flux in cyclonic and mode-water eddies in the Sargasso Sea. Deep Sea Res II 55:1360–1377

Green EP, Dagg MJ (1997) Mesozooplankton associations with medium to large marine snow aggregates in the northern Gulf of Mexico. J Plankton Res 19:435–447

Gutiérrez-Rodríguez A, Décima M, Popp BN, Landry MR (2014) Isotopic invisibility of protozoan trophic steps in marine food webs. Limnol Oceanogr 59:1590–1598

Hannides CCS, Popp BN, Landry MR, Graham BS (2009) Quantification of zooplankton trophic position in the North Pacific Subtropical Gyre using stable nitrogen isotopes. Limnol Oceanogr 54:50–61

Hannides CCS, Popp BN, Choy CA, Drazen JC (2013) Midwater zooplankton and suspended particle dynamics in the North Pacific Subtropical Gyre: a stable isotope perspective. Limnol Oceanogr 58:1931–1946

Hansen B, Bjornsen PK, Hansen PJ (1994) The size ratio between planktonic predators and their prey. Limnol Oceanogr 39:395–403

Haury LR (1988) Vertical distribution of *Pleuromamma* (Copepoda: Metridinidae) across the eastern North Pacific Ocean. Hydrobiologia 167:335–342

Hayward TL (1980) Spatial and temporal feeding patterns of copepods from the North Pacific Central Gyre. Mar Biol 58:295–309

Hetherington ED, Kurle CM, Ohman MD, Popp BN (2019) Effects of chemical preservation on bulk and amino acid isotope ratios of zooplankton, fish, and squid tissues. Rapid Commun Mass Spectrom 33:935–945

Hoen DK, Kim SL, Hussey NE, Wallsgrove NJ, Drazen JC, Popp BN (2014) Amino acid ^{15}N trophic enrichment factors of four large carnivorous fishes. J Exp Mar Biol Ecol 453:76–83

Landry MR, Décima M (2017) Protistan microzooplankton and the trophic position of tuna: quantifying the trophic link between micro- and mesozooplankton in marine food webs. ICES J Mar Sci 74:1885–1892

Landry MR, Brown SL, Rii YM, Selph KE, Bidigare RR, Yang EJ, Simmons MP (2008a) Depth-stratified phytoplankton dynamics in Cyclone *Opal*, a subtropical mesoscale eddy. Deep Sea Res II 55:1348–1359

Landry MR, Décima M, Simmons MP, Hannides CCS, Daniels E (2008b) Mesozooplankton biomass and grazing responses to Cyclone *Opal*, a subtropical mesoscale eddy. Deep Sea Res II 55:1378–1388

Legendre L, Rassoulzadegan F (1995) Plankton and nutrient dynamics in marine waters. Ophelia 41:153–172

Lorrain A, Graham B, Ménard F, Popp B, Bouillon S, van Breugel P, Cherel Y (2009) Nitrogen and carbon isotope values of individual amino acids: a tool to study foraging ecology of penguins in the Southern Ocean. Mar Ecol Prog Ser 391:293–306

Macko SA, Uhle ME, Engel MH, Andrusevich V (1997) Stable nitrogen isotope analysis of amino acid enantiomers by gas chromatography combustion/isotope ratio mass spectrometry. Anal Chem 69:926–929

Mahaffey C, Benitez-Nelson CR, Bidigare RR, Rii Y, Karl DM (2008) Nitrogen dynamics within a wind-driven eddy. Deep Sea Res II 55:1398–1411

Maiti K, Benitez-Nelson CR, Rii Y, Bidigare R (2008) The

influence of a mature cyclonic eddy on particle export in the lee of Hawaii. Deep Sea Res II 55:1445–1460
McAndrew PM, Bidigare RR, Karl DM (2008) Primary production and implications for metabolic balance in Hawaiian lee eddies. Deep Sea Res II 55:1300–1309
McClelland JW, Montoya JP (2002) Trophic relationships and the nitrogen isotopic composition of amino acids in plankton. Ecology 83:2173–2180
McGillicuddy DJ (2016) Mechanisms of physical-biological-biogeochemical interaction at the oceanic mesoscale. Annu Rev Mar Sci 8:125–159
McGowan JA, Walker PW (1979) Structure in the copepod community of the North Pacific Central Gyre. Ecol Monogr 49:195–226
McMahon KW, Thorrold SR, Elsdon TS, McCarthy MD (2015) Trophic discrimination of nitrogen stable isotopes in amino acids varies with diet quality in a marine fish. Limnol Oceanogr 60:1076–1087
Metges CC, Petzke KJ, Hennig U (1996) Gas chromatography combustion isotope ratio mass spectrometric comparison of *N*-acetyl- and *N*-pivaloyl amino acid esters to measure ^{15}N isotopic abundances in physiological samples: a pilot study on amino acid synthesis in the upper gastro-intestinal tract of minipigs. J Mass Spectrom 31:367–376
Möller KO, St John M, Temming A, Floeter J, Sell AF, Herrmann JP, Möllmann C (2012) Marine snow, zooplankton and thin layers: indications of a trophic link from small-scale sampling with the Video Plankton Recorder. Mar Ecol Prog Ser 468:57–69
Mompeán C, Bode A, Gier E, McCarthy MD (2016) Bulk vs. amino acid stable N isotope estimations of metabolic status and contributions of nitrogen fixation to size-fractionated zooplankton biomass in the subtropical N Atlantic. Deep Sea Res I 114:137–148
Mullin MM, Rau GH, Eppley RW (1984) Stable nitrogen isotopes in zooplankton: some geographic and temporal variations in the North Pacific. Limnol Oceanogr 29: 1267–1273
Nencioli F, Kuwahara VS, Dickey TD, Rii YM, Bidigare RR (2008) Physical dynamics and biological implications of a mesoscale eddy in the lee of Hawai'i: Cyclone Opal observations during E-Flux III. Deep Sea Res II 55: 1252–1274
Nielsen JM, Popp BN, Winder M (2015) Meta-analysis of amino acid stable nitrogen isotope ratios for estimating trophic position in marine organisms. Oecologia 178:631–642
Ohkouchi N, Chikaraishi Y, Close HG, Fry B and others (2017) Advances in the application of amino acid nitrogen isotopic analysis in ecological and biogeochemical studies. Org Geochem 113:150–174
Ohtsuka S, Böttger-Schnack R, Okada M, Onbé T (1996) In situ feeding habits of *Oncaea* (Copepoda: Poecilostomatoida) from the upper 250 m of the central Red Sea, with special reference to consumption of appendicularian houses. Bull Plankton Soc Japan 43:89–105
Oschlies A, Garçon V (1998) Eddy-induced enhancement of primary production in a model of the north Atlantic Ocean. Nature 394:266–269
Rau GH, Ohman MD, Pierrot-Bults A (2003) Linking nitrogen dynamics to climate variability off central California: a 51 year record based on $^{15}N/^{14}N$ in CalCOFI zooplankton. Deep Sea Res II 50:2431–2447
Rii YM, Brown SL, Nencioli F, Kuwahara V, Dickey T, Karl DM, Bidigare RR (2008) The transient oasis: nutrient-phytoplankton dynamics and particle export in Hawaiian lee cyclones. Deep Sea Res II 55:1275–1290
Seki MP, Polovina JJ, Brainard RE, Bidigare RR, Leonard CL, Foley DG (2001) Biological enhancement at cyclonic eddies tracked with GOES thermal imagery in Hawaiian waters. Geophys Res Lett 28:1583–1586
Sherin CK, Sarma V, Rao GD, Viswanadham R, Omand MM, Murty VSN (2018) New to total primary production ratio (f-ratio) in the Bay of Bengal using isotopic composition of suspended particulate organic carbon and nitrogen. Deep Sea Res I 139:43–54
Shulzitski K, Sponaugle S, Hauff M, Walter K, D'Alessandro EK, Cowen RK (2015) Close encounters with eddies: oceanographic features increase growth of larval reef fishes during their journey to the reef. Biol Lett 11: 20140746
Shulzitski K, Sponaugle S, Hauff M, Walter KD, Cowen RK (2016) Encounter with mesoscale eddies enhances survival to settlement in larval coral reef fishes. Proc Natl Acad Sci USA 113:6928–6933
Siegel DA, McGillicuddy DJ, Fields EA (1999) Mesoscale eddies, satellite altimetry, and new production in the Sargasso Sea. J Geophys Res Oceans 104:13359–13379
Steinberg DK, Silver MW, Pilskaln CH, Coale SL, Paduan JB (1994) Midwater zooplankton communities on pelagic detritus (giant larvacean houses) in Monterey Bay, California. Limnol Oceanogr 39:1606–1620
Steinberg DK, Silver MW, Pilskaln CH (1997) Role of mesopelagic zooplankton in the community metabolism of giant larvacean house detritus in Monterey Bay, California, USA. Mar Ecol Prog Ser 147:167–179
Ueda K, Morgan SL, Fox A, Gilbart J, Sonesson A, Larsson L, Odham G (1989) *D*-alanine as a chemical marker for the determination of streptococcal cell wall levels in mammalian tissues by gas chromatography negative ion chemical ionization mass spectrometry. Anal Chem 61: 265–270
Vaillancourt RD, Marra J, Seki MP, Parsons ML, Bidigare RR (2003) Impact of a cyclonic eddy on phytoplankton community structure and photosynthetic competency in the subtropical North Pacific Ocean. Deep Sea Res I 50: 829–847
Waite AM, Stemmann L, Guidi L, Calil PHR and others (2016) The wineglass effect shapes particle export to the deep ocean in mesoscale eddies. Geophys Res Lett 43: 9791–9800

Editorial responsibility: Sigrun Jónasdóttir, Charlottenlund, Denmark

Submitted: October 10, 2019; Accepted: April 16, 2020
Proofs received from author(s): May 24, 2020